

Розроблений комплексний метод підвищення терміну служби хрестовин стрілочних переводів, що базується на врахуванні поздовжнього профілю хрестовини, величини динамічних сил та нормальних напружень.

Удосконалено поздовжній профіль хрестовини марки 1/11 проекту 1740 методом виконання наплавки у польових умовах експлуатації. Уклони траєкторії після проходу середньостатичного колеса запропонованим профілем сягають 3,7‰, замість 10‰ у заводського профілю хрестовини.

Встановлено, що збільшення навантаження на хрестовину до 60 % за рахунок просадки під брусом хрестовини призводить до прискореного розладнання хрестовини, внаслідок виникнення втомних дефектів на поверхні кочення, при цьому витрати на експлуатацію хрестовини збільшуються у п'ять разів.

Проведено моделювання динамічної взаємодії рухомого складу із заводським та запропонованим поздовжніми профілями хрестовин. Розрахунки динамічних процесів нелінійної взаємодії рухомого складу залізниць із хрестовиною заводського профілю і профілю відновленого наплавкою показали, що величина сил у запропонованій хрестовині при швидкості руху 150 км/год є на 50 % нижчою порівняно із заводським поздовжнім профілем. При лінійному моделюванні динамічних добавок сил величина сил зменшується у запропонованого профілю до 30 %.

Розраховано графічним методом величини осьових моментів інерції та моментів опору у характерних перерізах хрестовини. Проведено оцінку напружено-деформованого стану хрестовини із використанням рівнянь п'яти моментів для нерозрізної балки на пружних точкових опорах. Встановлено, що напруження при статичному розрахунку хрестовини є невисокими і набагато меншими за гранично допустиму величину напружень для даної марки сталі. Тому можна стверджувати, що хрестовина працює під навантаженням за рахунок використання наявних резервів міцності

Ключові слова: хрестовина, стрілочний перевід, рухомий склад залізниць, поздовжній профіль, динамічні сили

THEORETICAL STUDY INTO EFFICIENCY OF THE IMPROVED LONGITUDINAL PROFILE OF FROGS AT RAILROAD SWITCHES

V. Kovalchuk
PhD*

E-mail: kovalchuk.diiit@gmail.com

M. Sysyn

PhD, Associate Professor

Department of planning and design of railway infrastructure

Dresden University of Technology

Hettnerstraße, 3/353, Dresden, Germany, D-01069

E-mail: mykola.sysyn@tu-dresden.de

Ju. Sobolevska

PhD, Associate Professor

Department of fundamental disciplines**

E-mail: sobolevskyy@gmail.com

O. Nabochenko

PhD*

E-mail: olganabochenko@gmail.com

B. Parneta

PhD, Associate Professor***

E-mail: f_termit@yahoo.com

A. Pentsak

PhD, Associate Professor***

E-mail: apentsak1963@gmail.com

*Department of rolling stock and track**

**Lviv branch of Dnipropetrovsk National University

of Railway Transport named after Academician V. Lazaryan

I. Blazhkevych str., 12a, Lviv, Ukraine, 79052

***Department of construction industry

Lviv Polytechnic National University

S. Bandery str., 12, Lviv, Ukraine, 79013

1. Introduction

The railroads of Ukraine currently operate more than 53 thousand railroad switches and fixed crossings. Most of them (98 %) are single regular railroad switches. Basic structures of railroad switches, which are common on the railroads of Ukrzaliznytsia after 1990, are the switches of type R65 M1/11 and 1/9, designed at the Technology Design Bureau

of the Central Directorate of the Ministry of Railroads (TDB CD MR), projects 1740 and 2215, laid on reinforced concrete bars. These basic models of switches have been significantly modified. Modifications included the structural components of the frog, fixing, or counter-rail. The main geometrical dimensions of the frogs, however, have remained unchanged.

Since the beginning of 2000, given the requirements to the railroads of Ukrzaliznytsia related to accelerating the

speed of freight and passenger trains, there has been a mismatch between the existing structures of the upper structure of the track and the new conditions of operation. The result of a comprehensive analysis of the state of the railroad facilities of Ukrzaliznytsia, it was found that the speed potential of railroad switches was insufficient for the implementation of the accelerated motion of trains. A growth in the freight load, increases in the speed of motion and in the axial loads, resulted in the reduced lifetime of crossing pieces. Failures of frogs have grown, caused by both wear and defects. In this case, a large proportion of crossing pieces were removed from tracks as a result of the formation of defects of the contact-fatigue character.

The organization of high-speed train motion on railroads requires the mandatory improvement and optimization of parameters of railroad switches [1]. They necessitate limiting the speed of train motion at stations to not faster than 120 km/h (when using conventional designs of switches with composite or one-piece cast crossing pieces). Therefore, it is not possible to implement high speeds of trains between stations (up to 160÷200 km/h) without resolving a task on increasing the speed of train motion at the railroad switches at stations [1].

Design features of railroad switches and crossing pieces create irregularities along the path of rolling wheels both in the vertical and horizontal planes. A length-wise and width-wise change in the design of a frog also changes a railroad track width, the rigidity of rail threads and the under-rail base under them. All this creates additional dynamic forces, which in some cases are of the impact character. They lead to the more rapid wear of metallic parts in railroad switches, consequently to the accumulation of residual deformations; they, therefore, require larger expenditures to maintain and repair.

The enhanced level of force interaction between bearing elements of a railroad switch and the motion parts of the rolling stock is one of the most important features in the operation of railroad switches. Thus, the magnitudes of dynamic forces of interaction at railroad switches can exceed by several times the level of dynamic forces along a regular track. These forces can cause premature failures and breakdown of structures. In the case of inconsistency between their capacity and operational loads or, vice versa, at the oversized capacity and rigidity of structures, there will occur the increased wear and failures of the rolling stock [2].

This in turn calls for increased requirements to railroad switches in terms of their strength, stability, reliability and longevity.

Therefore, the design of railroad switches in general, and separate components in particular, should always meet the requirements of operation and ensure the safety of train motion at established speeds. Designs of railroad switches must take into consideration operating conditions that are constantly changing, implement the modern achievements by domestic and foreign science and technology, and must match the level of world standards.

Studies [1, 2] established that the main driving factor that determines the formation of inertial forces of the unsprung masses is the vertical irregularity at the rolling surface zone of the crossing piece.

It is the characteristics of a given vertical irregularity for the system «track-carriage» that actually determine the level of dynamic force interaction between the rolling stock wheels and a track.

The formation of irregularities in the zone of grooved crossing pieces is known to be related, first, to the conditions under which the wheels roll from a rail wing to the core (or vice versa), which is accompanied by the transfer of pressure from the wheels to small contact areas of the rail wing and core. That is why at the section of rolling from a rail wing to a core (or vice versa), these elements undergo the most intensive wear. Work of the upper layers of metal is accompanied by the plastic deformations of creasing or flattening. Due to the high contact pressure, this zone accumulates defects of the contact character.

The facts that we specified indicate the need to intensify work in the field of extending the operation time of crossing pieces, increasing their wear resistance, as well as their resistance to defect formation.

2. Literature review and problem statement

The task on prolonging the operation time of frogs is addressed by many scientists at various research institutes in Ukraine and at leading research institutes of Germany, the Netherlands, France, and the Russian Federation. The task on prolonging the operation time of crossing pieces at railroad switches has been solved and is being solved at present in various ways. The most progressive methods to prolong a frog life cycle include:

- improvement of the existing designs and development of the new designs of frogs;
- improvement of the technology and the search for effective regulating additions and new grades of steels for the manufacture of frogs;
- strengthening of the frog rolling surface;
- improving the system of maintaining the rail equipment and development of the new methods, as well as improvement of the already existing methods, for restoring the frogs.

The improvement of existing designs, as well as the development of new designs, of crossing pieces at railroad switches imply the creation of a monolithic design of the frog. The first stage of this work was a transition from the rail-composite to the composite frogs of the one-piece cast type of core with a greater wear area of the rail wings parts. Recent years have seen the development of projects of one-piece cast frogs of brand 1/11 and 1/18, which are recommended for use at train running speeds up to 160 km/h [2].

Building a more monolithic design of the frog improves the performance and increases the resistance to dynamic and vibratory loads. That thereby significantly improves the operational characteristics of frogs and prolongs their service life, especially at high speeds of train motion. One-piece cast frogs have been widely used at the railroads of France and the United States [3].

The most promising direction in the development of frog design is constructing the frogs with a continuous rolling surface, that is, with movable elements. Such crossing pieces were laid at the roads of France. Later, the frog designs with movable elements were tested in Russia, the United States, France, Austria, Japan, Germany, England, and other countries [3]. Most of the examined structures had significant drawbacks, which is why they were discontinued. The best operational characteristics among all designs of frogs with movable elements were demonstrated by crossing pieces with a movable core. They are much better at satisfying

the requirements to frogs at running speeds of trains up to 200 km/h in the forward direction [3]. This circumstance explains a widespread use of crossing pieces with a movable core at high-speed lines in Japan and France.

Along with the development of new structures of frogs, there is a great body of work related to the improvement of geometrical parameters of existing structures. Researchers examine the longitudinal and transverse profiles of the rolling surfaces of wing rails and a core, dimensions and configuration of grooves, track width in a frog, as well as other parameters [4, 5].

The next stage is the improvement of the frog manufacturing technology. Engineers at the Dnieper turnout plant solve this task by blowing the steel with argon in the process of smelting [3]. In Japan, high manganese steel is smelted for frogs with a lowered content of phosphorus.

A significant impact on the resistance of crossing pieces is exerted by the micro- and macrostructure of metal. The grain size, the shape and orientation of crystals and the presence of inclusions affect the intensity of defect formation. The improvements in the micro- and macrostructure of steel include the casting of a core, machining of rolling surfaces, thermal treatment and search for effective alloying additives and new grades of steels to manufacture the frogs [3]. Engineers have conducted field testing of frogs alloyed with nickel, molybdenum, niobium, chrome, aluminum, titanium, boron, etc. [6, 7].

At present, the European Union and many railroads in the world mostly use frogs fabricated from the high manganese steel. Such a steel has the property of self-compaction, thereby operating well under conditions of elevated dynamic loads. During operation of crosspieces made of this steel, the rolling surfaces of wing rails and a core are given the strain hardening, which leads to a decrease in the intensity of abrasion and metal crushing. However, the resistance of frogs made of high manganese steel against the formation of contact-fatigue defects is insufficient at present. This gives rise to the search for new grades of steel to produce the crossing pieces at railroad switches. The European Union states have banned making the frogs from high manganese steels due to the environmental considerations.

The purpose of the pre-operational strengthening of rolling surfaces of wing rails and a core in the zone of a wheel rolling is to increase the rigidity of metal and, consequently, to reduce the intensity of abrasion and crushing. During experimental research the strengthening of the rolling surfaces of frogs was achieved by the following techniques: rolling with a roller, strain hardening, forging, spraying a layer of the more rigid metal [3]. However, these strengthening techniques have not produced desired results as using a roller, as well as forging, led to an intensive crushing of the rolling surface, and the application of other techniques resulted in that the thickness of the strengthened layer of metal was insufficient.

Significant effect can be achieved when strengthening the worn-out parts of wing rails and a core by a pulse load generated by the focused charge of an explosive [3, 6]. Researchers examined strengthening me-

thods with an explosion in different environments, as well as techniques for the phased strengthening.

Foreign engineers have achieved significant results in the field of strengthening the rolling surface of frogs. In the United States and Canada, they have designed and implemented industrial installations for the strengthening of frogs by the explosive wave. The required magnitude of strengthening is achieved in three cycles. The lifespan of a crossing piece increases by 2.5–3 times.

The operational time of railroad switches in general and frogs in particular is greatly affected by improving the maintenance of railroad switching equipment [7, 8], that is, the implementation of regular measures to maintain it. Such measures include: the introduction of a system aimed to control and inspect the frogs, the timely execution of works to maintain the frogs, comprehensive repair of crossing pieces under stationary conditions. However, these activities do not include a comprehensive approach to maintaining the system of railroad switching equipment and there are no defined rational variants for this system [7, 9]. This task can be resolved only when taking into consideration all the factors of influence and possible measures by using mathematical methods of optimization.

The main changes introduced to the design of composite frogs that are operated in Ukraine are the introduction of a bent-up connection of a rail part of the rail wing with the one-piece-cast instead of a direct connection. This technique is applied at nearly all variants of the modified switches of model 1740. At the same time, there are other variants of them (railroad switch Dn330) with a change in the rolling surface by the introduction of a 1/7 cross slope to the rail wing (that is, the so-called impact-free rolling surface forms). There are variants of the frog with a smaller elevation of the rail wing rolling surface at a cross-section of 20 mm from 6.7 mm to 4.7 mm (project U1740-06) [10, 11].

The results of research [5] into frogs of brand 1/11, project 1740, of different modifications, show that the number of frogs removed because of vertical wear of the core and wing rails is 57 %, 43 % are due to defects (Fig. 1). The largest quantity of the removed frogs relates to the factor of vertical wear of the core.

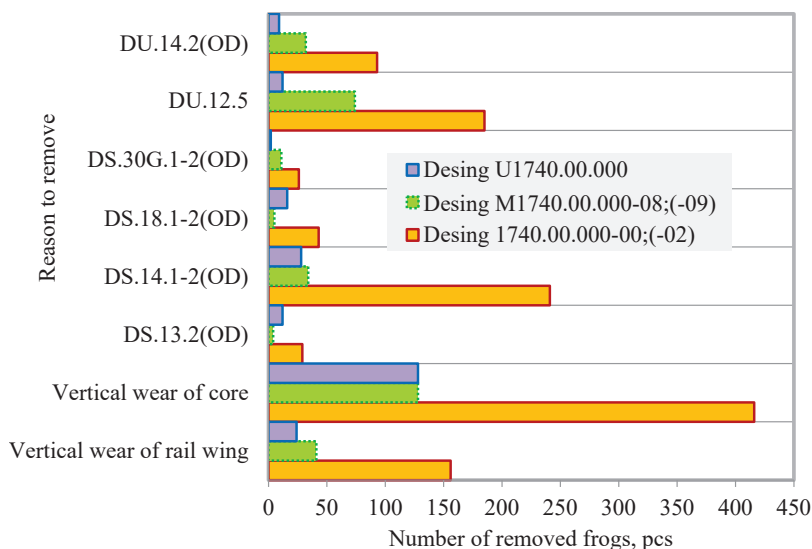


Fig. 1. Distribution of the removed frogs for project 1740 based on types of defects

The main reason for replacing the elements of frogs for project 1740 is the vertical wear of a core and a rail wing, 22 % and 11 %, respectively. In the zone where a wheel rolls from a rail wing onto a core, because of the increased dynamic interaction, defects relating to the crushing of a metal at the rolling surface of the rail wing and a core amount to 22 %. In addition to the defects specified above, a crossing piece has defects due to the metal piercing along the inline at the head because of drawbacks in the design, 14 %; crushing of the rolled layer of the metal that the cast part of a rail wing and a core is made of, 6 %.

One of the reasons for removing the elements of frogs for project M1740 is the vertical wear of a core, 35 %, and the vertical wear of a rail wing, 10 %. Defects relating to the crushing of a metal at the rolling surface of a rail wing and a core in the zone of rolling amount to 19 % due to the enhanced dynamic action. Defects of metal piercing along the inline at the head amount to 8 % because of drawbacks in the design; crushing of the rolled layer of the metal that the cast part of a rail wing and a core is made of accounts for 4 %.

For project 1740, the main cause for removing a frog is the vertical wear of a core, which accounts for 46 %. In this case, the vertical wear of a rail wing is 6 %, metal crushing at the rolling surface of a rail wing and a core accounts for 11 %, metal piercing along the inline at the head amount to 8 % because of drawbacks in the design.

Thus, it is a relevant and promising task to prolong the service life of crossing pieces, both in terms of ensuring train motion safety and economic expediency. The timely-made decision on the appropriateness of the continuation of using the existing projects of railroad switches and elements, as well as the implementation of experimental structures, would make it possible to significantly reduce the cost of railroad facilities. Prolonging the operation time of railroad switches by only 5 % ensures a saving of over UAH 10 million per year [12].

An analysis of research papers reveals that up to now the issue of improving the longitudinal profile of frogs has not received sufficient attention. However, given the technical condition of crossing pieces, the relevance of prolonging their life cycle has remained a promising task. To this end, it is necessary to design such a longitudinal profile, which would reduce the dynamic addition of forces, which exerts a direct influence on failures of frogs during operation.

3. The aim and objectives of the study

The aim of this work is to design and substantiate the effectiveness of using the improved longitudinal profile of crossing pieces at railroad

switches of brand 1/11, project 1740, in order to prolong the operation cycle of crossing pieces.

- To accomplish the aim, the following tasks have been set:
- to design a new longitudinal profile of the frog after the restoration by surfacing;
 - to construct a mathematical model for estimating the magnitude of a dynamic addition of forces on a frog;
 - to estimate the stressed-strained state of the frog employing the method of five moments.

4. Design of the new longitudinal profile of the frog

One of the methods to prolong the operation time of frogs at railroad switches is the method of surfacing [12, 13].

The technology of work execution and requirements to the choice of the material for the surfacing of frogs at railroad switches under field conditions are listed in the regulatory document [14]. The result of executing the work on surfacing, the geometry of an industrially produced profile can be modified.

Therefore, we propose the improved longitudinal profile of the frog (Fig. 2).

In a given profile, a height of the core against the cross section of 20 mm was increased to 3 mm instead of 2 mm for a standard profile of the frog. Such an increase is maintained to the cross section of the frog core equal to 30 mm. The profile of the core subsequently decreases to become equal to 0 in the cross section of 60 mm.

The longitudinal profile of wing rails in the cross section of 20 mm decreases to 4.0 mm instead of 6.7 mm for a standard profile; the longitudinal profile before crossing the core decreases to 0 mm.

Employing the procedure given in paper [5] we derived a motion trajectory of the center of mass of the wheel over the standard and the proposed profiles (Fig. 3).

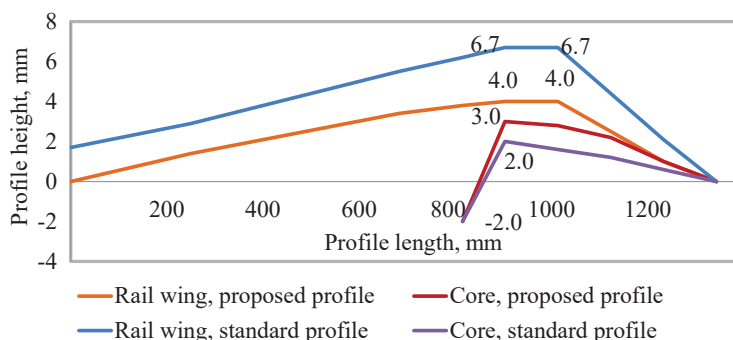


Fig. 2. Standard and proposed longitudinal profiles of the frog

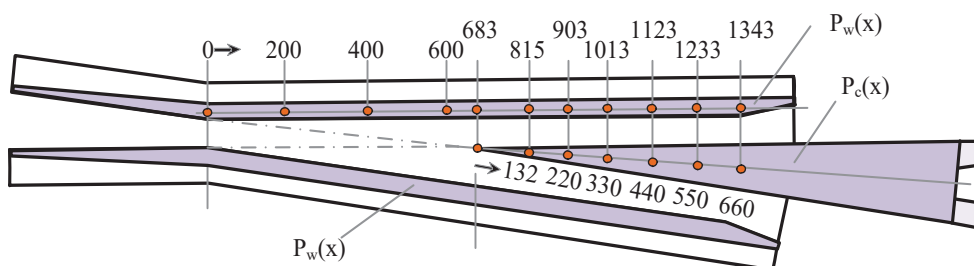


Fig. 3. Longitudinal profile of the frogs of brand 1/11

In the general form, a trajectory of the wheel motion over a frog can be recorded in the form of dependence:

$$y(x) = f\{P(x), W(x), \delta\}, \quad (1)$$

where $y(x)$ is the trajectory of the wheel that rolls over a frog in the vertical plane; $P(x)$ is the frog profile; $W(x)$ is the transverse profile of the wheel brace; δ is the magnitude of the gap between a working edge of the wheel and a working edge of the rail wing (core).

The longitudinal profile of the frog will be represented in the form of two linear functions: $P_w(x)$ is the longitudinal profile of wing rails and $P_c(x)$ is the longitudinal profile of a core. Fig. 3 shows abscissas of functions $P_w(x)$ and $P_c(x)$ that were accepted to derive the motion trajectory of the center of mass of the wheel over the frog of brand 1/11.

The trajectory that forms when a standard wheel rolls over a regular profile of the frog (Fig. 4) acquires a wave-like shape with a maximum increase at a distance of 400 mm from the throat of the frog +0.8 mm and a maximum decrease of -1.1 mm in the cross section of the core of 30 mm. The proposed profile has a maximum increase, in the cross section of 400 mm, of +0.3 mm, and a maximal decrease is -0.5 mm. The slopes of trajectory after a standard wheel rolls over a typical profile of the frog amount to 10 ‰ instead of 3.7 ‰ for the proposed profile of the frog.

The power function of the seventh order defined coefficients of the polynomials that approximate the motion trajectory of a standard wheel over a longitudinal profile of the frog of brand 1/11.

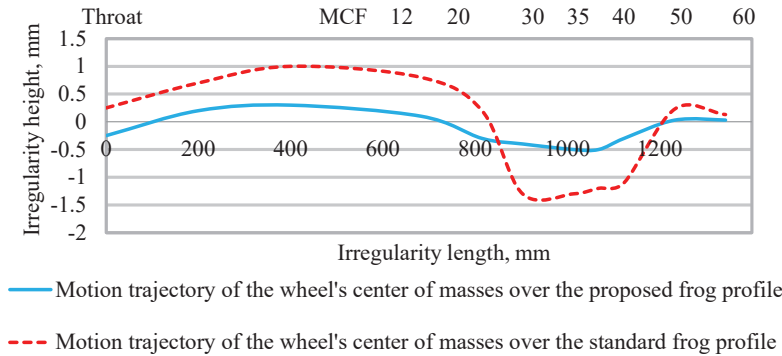


Fig. 4. Motion trajectory charts of the wheel's center of masses over the longitudinal profiles

For a standard profile, coefficients of the polynomial acquire the following values: $a_0=0.2484$, $a_1=0.017$, $a_2=0.0002$, $a_3=5 \cdot 10^{-7}$, $a_4=-9 \cdot 10^{-10}$, $a_5=6 \cdot 10^{-13}$, $a_6=-2 \cdot 10^{-16}$, and for the improved profile, restored by the method of surfacing: $a_0=-0.2499$, $a_1=0.0064$, $a_2=-4 \cdot 10^{-5}$, $a_3=1 \cdot 10^{-7}$, $a_4=-2 \cdot 10^{-10}$, $a_5=1 \cdot 10^{-13}$, $a_6=-4 \cdot 10^{-17}$.

4. Construction of a mathematical model and estimation of the magnitude of a dynamic addition of forces on the frog

The motion of rolling stock wheels over the frog at a railroad switch has a complicated character. At motion over a rail wing as a result of the brace end, the wheel moves in the vertical plane. Additional forces of inertia occur in this case, acting on the rolling stock and the track [15, 16]. To model the dynamic interaction between a frog at a railroad

switch and the rolling stock, we adopted the following models (Fig. 5):

- a model of the car is taken to be a generalized mechanical system that is composed of two inertial bodies – the over spring mass and the unsprung mass, and represents the passage of one axle of the carriage;

- a model of the frog is a model composed of the continual inertial Euler beams with a mass concentrated in the axes of the beams.

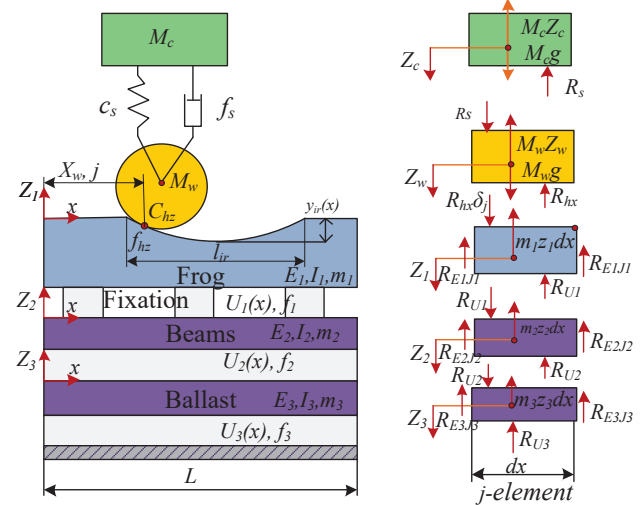


Fig. 5. Estimation scheme of interaction between a frog and the rolling stock

The beams are placed one on one; they are separated by elastic continual layers, which correspond to the Winkler base and possess the viscous-dissipative properties. The lower beam is placed at a stationary base [17–19]. Each of the beams corresponds to the structural elements: a frog, a sleeper with fixation, a ballast layer with soil roadbed. The action of separate sleepers is described through the introduction to the upper connecting layer of gaps with a small value of rigidity and damping [20, 21].

Simulation of the dynamic interaction between a track and the rolling stock is conducted by solving a system of differential equations (1) according to the accepted estimation scheme (Fig. 5).

The derivation of separate equations is not included since each of the elements of the system is a standard one; these elements can be found in the scientific literature [21, 22].

$$M_c \frac{d^2 z_c(t)}{dt^2} + C_s (z_c(t) - z_w(t)) + f_s \left(\frac{dz_c(t)}{dt} - \frac{dz_w(t)}{dt} \right) = M_c g;$$

$$M_w \frac{d^2 z_w(t)}{dt^2} + C_{hz} (z_w(t) + y_{ir}(x_K) - z_1(x_{ir}, t)) + f_{hz} \left(\frac{dz_{ir}(t)}{dt} + \frac{dy_{ir}(x_w)}{dt} - \frac{dz_1(x_w, t)}{dt} \right) = C_s (z_c(t) - z_w(t)) + f_s \left(\frac{dz_c(t)}{dt} - \frac{dz_w(t)}{dt} \right) + M_w g;$$

$$\begin{aligned}
 & E_1 I_1 \frac{\partial^4 z_1(x,t)}{\partial x^4} + m_1 \frac{\partial^2 z_1(x,t)}{\partial t^2} + \\
 & + f_1 \left(\frac{\partial z_1(x,t)}{\partial t} - \frac{\partial z_2(x,t)}{\partial t} \right) + U_1(x) (z_1(x,t) - z_2(x,t)) = \\
 & = \left(C_{hz} (z_w(t) + y_{ir}(x_K) - z_1(x_w,t)) + \right. \\
 & \left. + f_{hz} \left(\frac{dz_w(t)}{dt} + \frac{dy_{ir}(x_K)}{dt} - \frac{dz_1(x_w,t)}{dt} \right) \right); \quad (2) \\
 & E_2 I_2 \frac{\partial^4 z_2(x,t)}{\partial x^4} + m_2 \frac{\partial^2 z_2(x,t)}{\partial t^2} + \\
 & + f_2 \left(\frac{\partial z_2(x,t)}{\partial t} - \frac{\partial z_3(x,t)}{\partial t} \right) + U_2(x) (z_2(x,t) - z_3(x,t)) = \\
 & = U_1(x) (z_1(x,t) - z_2(x,t)) + f_1 \left(\frac{\partial z_1(x,t)}{\partial t} - \frac{\partial z_2(x,t)}{\partial t} \right); \\
 & E_3 I_3 \frac{\partial^4 z_3(x,t)}{\partial x^4} + m_3 \frac{\partial^2 z_3(x,t)}{\partial t^2} + \\
 & + f_3 \frac{\partial z_3(x,t)}{\partial t} + U_3(x) z_3(x,t) = \\
 & = U_2(x) (z_2(x,t) - z_3(x,t)) + f_2 \left(\frac{\partial z_2(x,t)}{\partial t} - \frac{\partial z_3(x,t)}{\partial t} \right).
 \end{aligned}$$

Denotations that are accepted for the scheme in Fig. 5 and for the system of differential equations (2) are: M_c is the over spring mass of the car, reduced to one wheel; C_s is the rigidity of suspension, reduced to one wheel; f_s is the damping in the suspension, reduced to one wheel; M_w is the unsprung mass of the car, reduced to one wheel; C_{hz} is the rigidity in the contact between a wheel and a rail; f_{hz} is the damping in the contact between a wheel and a rail; m_1, m_2, m_3 are the masses of a rail, sleepers with fixation, a ballast layer of roadbed, reduced to the axes of respective beams along the track; z_c, z_w, z_1, z_2, z_3 are the displacements of masses of the car, of the wheel, of the rail, sleepers with fixation, of the ballast layer of roadbed, respectively; E_1, E_2, E_3 are the elasticity moduli of respective elements, reduced to the axes of the corresponding beams; I_1, I_2, I_3 are the moments of inertia of respective elements reduced to the axes of corresponding beams; $U_2(x), U_3(x)$ are the functions of the roadbed coefficient, which accounts for the possibility of the existence of non-uniform elasticity in the ballast or a soil bed, that is, a force irregularity; $U_1(x)$ is the piecewise function, which shows a change

in the roadbed coefficient in a layer of sealing and is null in the intra-sleeper space; f_2, f_3 is the damping in the connecting elements of sleepers, the ballast layer, and a soil bed; f_1 is the damping in the sealing layer (it is null in the intra-sleeper space); l_s is the distance between the axes of sleepers; y_{ir} is the depth of a geometrical isolated irregularity on the rail; l_{ir} is the length of a geometrical isolated irregularity on the rail; R_i are the reactions of joints between elements of the systems and the rolling stock that possess elastic and damping properties; g is the acceleration of free fall.

The first two equations of system (2) represent the displacement of discrete masses, the last three – the vertical displacements of continual beams. The system consists of two ordinary differential equations and three equations in partial derivatives. It is proposed to solve such a system of equations using a numerical technique employing the Gün's method [23] for integration over a preset time interval, which corresponds to the passage of the external load over the entire length of the beam, including an irregularity.

Practical implementation of the calculation is performed using the Matlab 10 software package [24].

As an example of calculation, we shall demonstrate results of modeling the motion of the car along a section of the track with a length of 22 m, which includes the frog. When performing the calculation, the following initial data were assigned: $M_c = 11600$ kg; $M_w = 990$ kg; $m_1 = 65$ kg/m; $m_2 = 250$ kg/m; $m_3 = 700$ kg/m; $E_1 = 2.1 \cdot 10^{11}$ N/m²; $I = 3,548 \cdot 10^{-8}$ m⁴; $C_s = 80 \cdot 10^9$ N/m. All magnitudes of the efforts along the frog that occur in connecting elastic-dissipative layers of the model, which match the fixation, ballast, and a soil bed, are reduced to be considered as the intensity of load, or a force of action per 1 m along the axis of the frog (Fig. 6). At the point of contact between the wheel and the frog the efforts change continuously; in this case, they increase over an irregularity depending on the parameters of the irregularity.

In order to compare the forces of dynamic interaction between the rolling stock and a frog, we set the motion speed from 60 km/h to 150 km/h. The frog has a geometrical irregularity when a wheel moves over a standard longitudinal profile of the frog and the frog profile optimized by surfacing. Distance between the axes of the beams is taken to be 0.55 m.

Results of the linear and nonlinear simulation of the force of a wheel action on the frog at the point of their contact at different longitudinal profiles of frogs and at different motion speed of the railroad rolling stock are shown in Fig. 7.

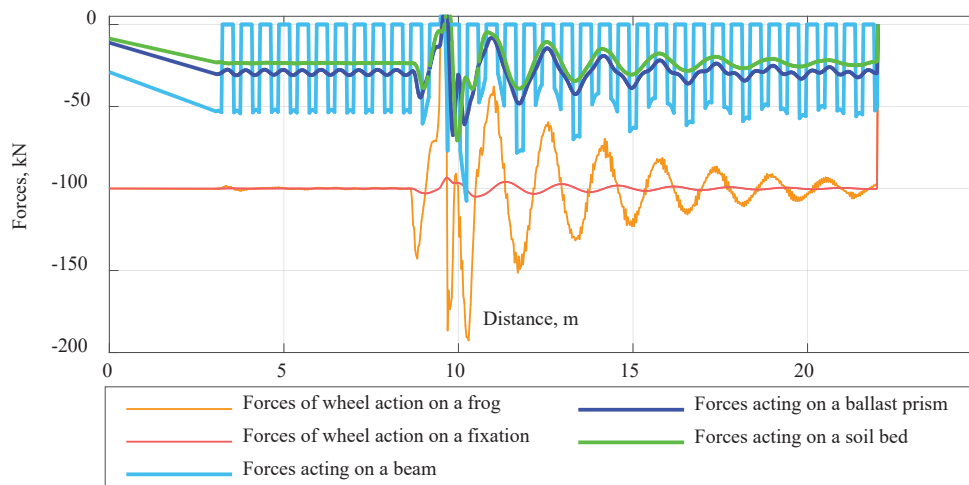


Fig. 6. Parameters of interaction between a track and the rolling stock when passing over an irregularity on the frog

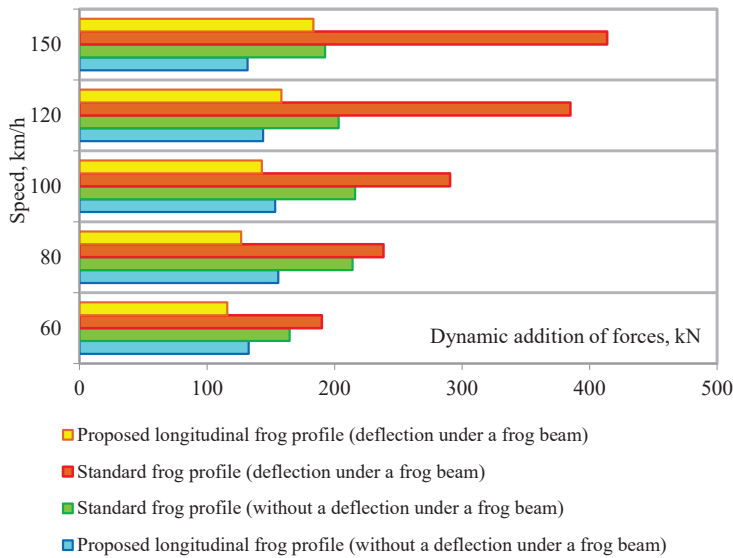


Fig. 7. Comparison of the force of a wheel action on the frog for a standard profile and the surfaced profile

Fig. 7 shows that when modeling the interaction between a frog and the rolling stock without a deflection under a frog beam the maximal magnitude of a dynamic addition of forces occurs at the rolling stock motion speed of 100 km/h; the magnitude for a standard profile is 216.1 kN; for the profile restored by the surfacing method, it is 153.4 kN.

The result of assigning a deflection under a frog beam is the derived non-linear model. The magnitude of interaction forces at a speed of 150 km/h for a standard profile is 413.7 kN; for the profile restored by the surfacing method, it is 183.4 kN.

Thus, the magnitude of forces for the proposed frog at a motion speed of 150 km/h is 50 % lower compared with a standard longitudinal profile.

At linear simulation of the dynamic addition of forces, the magnitude for the proposed profile decreases by up to 30 % compared to a standard one.

Based on data from [20], the influence of operational factors on the disarrangement of all elements of the track was established, considering even a damage to the elements of the upper structure of the track. In this case, the impact of operational factors can be significantly strengthened depending on the geometrical state of the track. The organization ORE conducted a number of studies to determine the influence of these factors. The Committee ORE D141 improved a quantitative method of calculation, which assumes that a disarrangement of the track geometry is a function of the degree of load according to formula (3):

$$E = kT^\alpha P^\beta V^\gamma, \tag{3}$$

where E is the expenditure rise in the track operation due to the disarrangement after restoration or following the latest maintenance operation; T is the passed tonnage; P is the full axial load (static+dynamic); V is the motion speed; k , α , β , γ are constants. The parameters α , β were determined empirically by the ORE committees D141 and D17. Values for the disarrangement factors for a damage of the frog surface are $\alpha = 1.0$ and $\beta = 3.5$.

The share of ratio of maximum dynamic forces, arising in a standard profile of the frog, to the proposed profile, in linear

modeling, is 1.4; in this case, the expenditure factor is 3.2. At nonlinear modeling, the share of ratio of maximum dynamic forces, arising in a standard profile of the frog, to the proposed profile, is 2.26; in this case, the expenditure factor is 17.2. Therefore, increasing the load leads to the accelerated disarrangement of the frog, due to the occurrence of fatigue defects at the frog rolling surface. This in turn results in an increased costs of frog operation at railroad switches.

The cost is inversely proportional to the passed load at the point of current maintenance. Consequently, the ratio of expenditure $E_{216.1}/E_{153.4}$ is equal to:

$$\frac{E_{216.1}}{E_{153.4}} = \left[\frac{P_{216.1}}{P_{153.4}} \right]^{\beta/\alpha} \tag{4}$$

In practice, the cost ratios for the distribution of load should be derived from formula:

$$\frac{E_2}{E_1} = \frac{\sum_i n_{2i} P_i^{\beta/\alpha}}{\sum_i n_{1i} P_i^{\beta/\alpha}}, \tag{5}$$

where n_{1i} , n_{2i} is the share of impact of one group of load; P_i is the mean level of force load on the group of load for a standard profile and the proposed profile.

5. Development of a procedure for calculating the stressed-strained state of the frog using the method of five moments

We shall accept the estimated scheme of the frog in the form of a continuous beam with a variable cross section, which rests on the bars in 6 cross sections located at equal distances from each other (Fig. 8).

One of the supports is considered to be the hinge-fixed one to receive the axial load, the remaining to be the hinge-movable ones [25]. To form the main system, we place the hinges in the beam cross section over the intermediate supports.

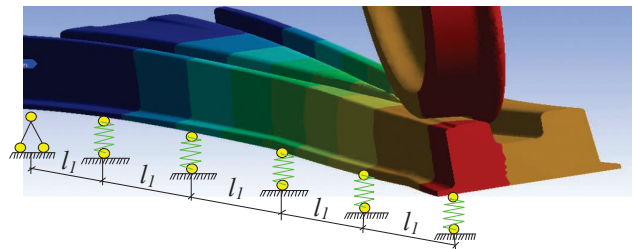


Fig. 8. Estimated scheme of the frog

The unknowns to the method of forces at such a choice of the main system are the bending moments in the anchor cross sections of the beam: $X_1 = M_1$, $X_2 = M_2$, $X_3 = M_3$, $X_4 = M_4$.

It is believed that the beam has a constant cross-section within the limits of one run.

It is assumed that the base of the frog is elastic due to the gasket and the displacements of supports proportional to support reactions [25]:

$$y_n = k_n R_n. \tag{6}$$

In this case, we consider that complete reaction R_n in the support number n is derived as the sum of reaction of the statically determined beam due to the action of known load R_n^0 , applied within the limits of the run, and the reaction due to the action of supporting moments, not known in advance:

$$R_n = R_n^0 - (M_n - M_{(n-1)})/l_n + (M_{(n+1)} - M_n)/l_{(n+1)}. \quad (7)$$

As a result of the displacement of supports with numbers $(n-1)$, n and $(n+1)$ by y_{n-1} , y_n and y_{n+1} , respectively, the beams of the main system with numbers n and $(n+1)$ would rotate at angles that are calculated from formula:

$$\begin{aligned} \theta_n &= \frac{y_n - y_{n-1}}{l_n}, \\ \theta_{n+1} &= \frac{y_{n+1} - y_n}{l_{n+1}}. \end{aligned} \quad (8)$$

The mutual turning angle of cross sections in support n will equal $\theta_{n+1} - \theta_n$. The equations of the three moments take the following form:

$$X_{n-1} \frac{l_n}{l_n} + 2X_n \left(\frac{l_n}{l_n} + \frac{l_{n+1}}{l_{n+1}} \right) + X_{n+1} \frac{l_{n+1}}{l_n} = -6E(\theta_{n+1} - \theta_n), \quad (9)$$

where $n=1...4$.

After substituting expressions for turning angles (8) with respect to (6) and (7) into equations of three moments (9), we obtain an equation of five moments.

$$\begin{aligned} &X_1 \left[2 \left(\frac{l_1}{l_1} + \frac{l_2}{l_2} \right) + 6E \frac{k_0}{l_1^2} + 6Ek_1 \left(\frac{1}{l_1} + \frac{1}{l_2} \right)^2 + 6Ek_2 \frac{1}{l_1^2} \right] + \\ &+ X_2 \left[\frac{l_2}{l_2} - 6Ek_1 \frac{1}{l_2} \left(\frac{1}{l_1} + \frac{1}{l_2} \right) - 6Ek_2 \frac{1}{l_2} \left(\frac{1}{l_2} + \frac{1}{l_3} \right) \right] + 6E \frac{k_2}{l_2 l_3} X_3 = \\ &= -6E \left(\Delta_{1F} - k_1 \left(\frac{1}{l_1} + \frac{1}{l_2} \right) R_1^0 + \frac{k_2}{l_2} R_2^0 + \frac{k_0}{l_1} R_0^0 \right). \\ &X_1 \left[\frac{l_2}{l_2} - 6Ek_1 \cdot \frac{1}{l_2} \left(\frac{1}{l_1} + \frac{1}{l_2} \right) - 6Ek_2 \cdot \frac{1}{l_2} \left(\frac{1}{l_2} + \frac{1}{l_3} \right) \right] + \\ &+ X_2 \left[2 \left(\frac{l_2}{l_2} + \frac{l_3}{l_3} \right) + 6Ek_1 \frac{1}{l_2^2} + 6Ek_2 \left(\frac{1}{l_2} + \frac{1}{l_3} \right)^2 + 6Ek_3 \frac{1}{l_3^2} \right] + \\ &+ X_3 \left[\frac{l_3}{l_3} - 6Ek_2 \cdot \frac{1}{l_3} \left(\frac{1}{l_2} + \frac{1}{l_3} \right) - 6Ek_3 \frac{1}{l_3} \left(\frac{1}{l_3} + \frac{1}{l_4} \right) \right] + \\ &+ X_4 \left[6E \frac{1}{l_3 l_4} k_3 \right] = -6E \left(\Delta_{2F} + \frac{k_1}{l_2} R_1^0 - k_2 \left(\frac{1}{l_2} + \frac{1}{l_3} \right) R_2^0 + \frac{k_3}{l_3} R_3^0 \right). \\ &X_1 \left(6E \frac{1}{l_2 l_3} k_2 \right) + X_2 \left[\frac{l_3}{l_3} - 6Ek_2 \frac{1}{l_3} \left(\frac{1}{l_2} + \frac{1}{l_3} \right) - 6Ek_3 \frac{1}{l_3} \left(\frac{1}{l_3} + \frac{1}{l_4} \right) \right] + \\ &+ X_3 \left[2 \left(\frac{l_3}{l_3} + \frac{l_4}{l_4} \right) + 6E \frac{1}{l_3^2} k_2 - 6Ek_3 \left(\frac{1}{l_3} + \frac{1}{l_4} \right)^2 + 6Ek_4 \frac{1}{l_4^2} \right] + \\ &+ X_4 \left[\frac{l_4}{l_4} - 6E \frac{1}{l_4} k_3 \left(\frac{1}{l_3} + \frac{1}{l_4} \right) - 6E \frac{1}{l_4} k_4 \left(\frac{1}{l_4} + \frac{1}{l_5} \right) \right] = \\ &= -6E \left(\Delta_{3F} + \frac{1}{l_3} k_2 R_2^0 - k_3 R_3^0 \left(\frac{1}{l_3} + \frac{1}{l_4} \right) + \frac{1}{l_4} k_4 R_4^0 \right). \end{aligned}$$

$$\begin{aligned} &X_2 6E \frac{k_3}{l_3 l_4} + X_3 \left[\frac{l_4}{l_4} - 6E \frac{1}{l_4} k_3 \left(\frac{1}{l_3} + \frac{1}{l_4} \right) - 6Ek_3 \frac{1}{l_4} \left(\frac{1}{l_3} + \frac{1}{l_4} \right) \right] + \\ &+ X_4 \left[2 \left(\frac{l_4}{l_4} + \frac{l_5}{l_5} \right) + 6E \frac{k_3}{l_4^2} + 6Ek_4 \left(\frac{1}{l_4} + \frac{1}{l_5} \right)^2 + 6E \frac{k_5}{l_5^2} \right] = \\ &= -6E \left(\Delta_{4F} + \frac{k_3}{l_4} R_3^0 - k_4 R_4^0 \left(\frac{1}{l_4} + \frac{1}{l_5} \right) + \frac{k_5}{l_5} R_5^0 \right), \end{aligned}$$

where Δ_{iF} is the displacement of the main system in the directions of removed joints due the action of the preset external load (or mutual turning angles of supporting cross sections of the main system due to the action of the preset external load); l_n is the distance between supports that hold the frog; I_n are the axial moments of inertia of the transverse intersections of the frog; k is the frog base rigidity; E is the modulus of elasticity of the frog metal; R_n is the reaction of the support under load.

Based on the proposed mathematical model, we determined the bending moments and the largest normal stresses arising in the frog because of the action of statically applied amplitude values for the interaction forces between a wheel and a frog.

To determine the maximum normal stresses at bending, rigidity of the frog base was accepted as $k=7.5 \cdot 10^7$ kN/m, modulus of elasticity of the frog metal – $E=2.1 \cdot 10^5$ MPa.

Determining the magnitudes of axial moments of inertia of the frog, brand 1/11, project 1740, was conducted by a graphical method using the CAD software.

Parameters of geometrical characteristics of the frog are given in Table 1.

Table 1
Geometrical characteristics of the frog

Geometrical characteristics	Characteristic cross sections of the frog					
	10	20	30	40	50	60
Axial moments of inertia, cm ⁴	9609	10130	10070	10226	11110	12100
Resistance moments, cm ³	1050	1083	1100	1075	1118	578

The maximum values of the bending moments for a standard profile at a dynamic addition of force of 216.1 kN are 15.59 kNm; at 413.7 kN, the bending moment is equal to 33.47 kNm. For the profile improved by the method of surfacing at a dynamic addition of force of 153.4 kN, magnitude of the maximum bending moment is 10.67 kNm; at 183.4 kN – 14.85 kNm.

Given the calculated values for the bending moments and geometrical characteristics of the frog, we shall calculate normal stresses from formula:

$$\sigma = \frac{M}{W}, \quad (10)$$

where M is the bending moment; W is the moment of resistance of the frog cross section.

We determined, for the maximum values of bending moments, the maximum normal stresses (Fig. 9) arising during action of a vertical load for a standard profile and the proposed profile of the frog.

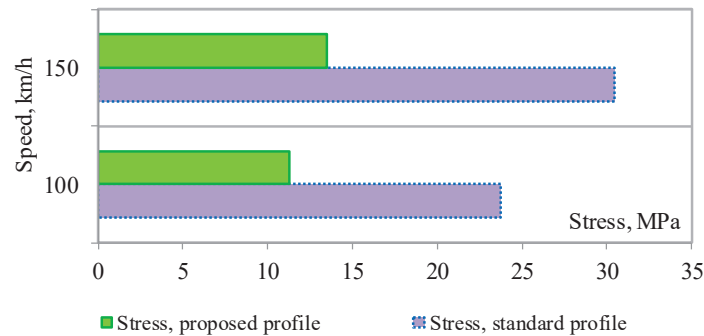


Fig. 9. Distribution of normal stresses and maximum bending moments in the cross section of the frog core of 35 mm

The results of calculation of the stressed state of the frog showed that a stress of 33.47 MPa is caused by a freight car at a maximum bending moment in the cross section of the frog of 35 mm, brand 1/11, project 1740. Therefore, the stresses at the static calculation of the frog are low and are much smaller than the maximum permissible magnitude of stress for a given grade of steel, which is 210 MPa according to technical specifications [14].

7. Discussion of study results aimed to evaluate the state of the strength of the frog at railroad switches

Large dynamic forces cause intensive wear of the frog elements (wing rails, cores), which reduces their service life and contributes to the development of defects in sleepers, which leads to cracking. In order to prolong the time of operation of frogs, it is recommended to use a method of surfacing with a simultaneous change in the longitudinal profile. At the change in the longitudinal profile, it is necessary to achieve the trajectory of a wheel motion that is close to rectilinear. It is necessary to ensure the largest length of the rolling zone, which would make it possible to increase the contact area between a wheel and a frog. It is necessary to distribute the force of the impact of the wheel against the core for a larger area and to ensure rolling the wheels at the smallest permissible angle to the elements of the railroad switch.

The ORE D141 committee established impact factors of the disarrangement of the frog geometry on the cost of regular maintenance. At a share of the ratio of maximum dynamic forces, arising in a standard profile of the frog, to the proposed profile, at linear modeling, which is 1.4, the expenditure factor according to the ORE D141 procedure is 3.2. At nonlinear modeling, the ratio of forces is 2.26; the expenditure factor, however, amounts to 17.2. Therefore, increasing the load leads to the accelerated disarrangement of a frog, due to the occurrence of fatigue defects at the rolling surface. This in turn results in the increased costs of operation of frogs at railroad switches.

The magnitude of forces in a contact between a wheel and a frog depends on parameters of a vertical irregularity in the zone where the rolling stock wheels roll over a frog. Determining the level of force workload on the railroad switches does not allow employing the calculation procedures that are used in determining the interaction forces for a typical track. Until recently, no any generally recognized method was developed, nor proposed, for the calculation of dynamic forces that arise within the limits of railroad switches or separate parts. Respective calculations most often employed flat

estimation schemes in the form of a system of concentrated masses, interconnected by elastic-dissipative links. At the same time, many similar calculation schemes were not precise enough to reflect the actual conditions for the interaction of the system «track-carriage».

The determined stressed state of the frog at static calculation made it possible to establish that the level of stresses is low and is much smaller than the maximum permissible magnitude of stress for a given grade of steel. Therefore, we can argue that the frog works under a load at the expense of existing reserve of strength.

The drawbacks of the study conducted are in that the derived criteria are based on the optimization of only the longitudinal profile of wing rails and a core of the frog, as well as on the estimation of maintenance costs at the occurrence of faults under the action of vertical dynamic loads. In addition, important factors when optimizing the frogs are the shape and area of the contact surface and the estimation of the frog disarrangement due to contact stresses. Therefore, in the future it is necessary to continue improving the comprehensive procedure for prolonging the life cycle of frogs, taking into consideration the above-mentioned factors that were not accounted for.

8. Conclusions

1. To prolong the time of operation of frogs at railroad switches, it is recommended to use the method of surfacing with a simultaneous change in the longitudinal profile of the frog, in which the slopes of a trajectory after the passage of a wheel with an average statistical wear should be equal to 3.7 ‰ instead of 10 ‰ for a standard profile of the frog.

Coefficients of the polynomials that approximate the motion trajectory of an average statistical wheel along the longitudinal profiles of the frog, brand 1/11, for a standard profile, are: $a_0=0.2484$, $a_1=0.017$, $a_2=0.0002$, $a_3=5 \cdot 10^{-7}$, $a_4=-9 \cdot 10^{-10}$, $a_5=6 \cdot 10^{-13}$ and $a_6=-2 \cdot 10^{-16}$; for the improved profile, restored by the surfacing method, they are $a_0=-0.2499$, $a_1=0.0064$, $a_2=-4 \cdot 10^{-5}$, $a_3=1 \cdot 10^{-7}$, $a_4=-2 \cdot 10^{-10}$, $a_5=1 \cdot 10^{-13}$ and $a_6=-4 \cdot 10^{-17}$.

2. The developed integrated algorithm for determining the dynamic interaction between the rolling stock and a frog made it possible to establish the scientific basis for improving the operation time of frogs at railroad switches. The magnitude of dynamic additions of forces for the proposed frog at the motion speed of 150 km/h is 50 % lower compared with a standard longitudinal profile. At linear modeling of dynamic additions of forces, the magnitude of forces decreases for the proposed profile to 30 %.

Increasing the load on the frog to 60 % at the expense of a deflection under the frog bar accelerates the disarrangement of the frog due to the occurrence of fatigue defects at the rolling surface, while the share of expenses for the operation of the frog increases in this case by five times.

3. The determined stressed state of the frog at static calculation using the method of five moments allowed us to

establish that the level of stresses is low and is much smaller than the maximum permissible magnitude of stress for a given grade of steel. Therefore, it can be argued that the frog works under a load at the expense of existing reserve of strength. Maximum normal stresses at the preset initial data in the frog cross section of 35 mm, brand 1/11, project 1740, are 33.47 MPa.

References

- Rybkin V. V., Panchenko P. V., Tokariev S. O. Istorychnyi analiz teoretychnykh ta eksperymentalnykh doslidzhen dynamiky kolyvi, strilochnykh perevodiv ta rukhomoho skladu // Zbirnyk naukovykh prats Donetskoho in-tu zalizn. tr-tu. 2012. Issue 32. P. 277–288.
- Danilenko E. I., Kutah A. P., Taranenko S. D. Strelochnye perevody zheleznyh dorogo Ukrainy. Kyiv: Kievskiy institut zhelezno-dorozhnogo transporta, 2001. 296 p.
- Instruktsiya z ulashtuvannia ta utrymannia kolyvi zaliznyts Ukrainy / Danilenko E. I., Orlovskiy A. M., Kurhan M. B., Yakovliev V. O. et. al. Kyiv: «NVP Polihrafservis», 2012. 395 p.
- Orlovskiy A. M., Kalenyk K. L., Kovalchuk V. V. Doslidzhenia pozdovzhnoho profilu zhorstkykh khrestovyn na zalizobetonnykh brusakh // Visnyk Dnipropetr. nats. un-tu zal. transp. im. ak. V. Lazariana. 2012. Issue 41. P. 130–135.
- Geometrische Optimierung von Weichenherzstücken / Gerber U., Sysyn M. P., Kowaltschuk W. W., Nabotschenko O. S. // EIK Eisenbahningieur kompendium. Euralpres. Deutschland, Hamburg, 2017. P. 229–240.
- Esveld C. Modern railway track. 2nd ed. MRT-Production, 2001. 653 p.
- Kovalchuk V., Bal O., Sysyn M. Development of railway switch frog diagnostics system // 6th International Scientific Conference organized by Railway Research Institute and Faculty of Transport of Warsaw University of Technology. Warsaw, 2017.
- Gerber U., Fengler W., Zoll A. Das Messsystem ESAH-M // In: EIK – Eisenbahningenieurkalender Jahrbuch für Schienenverkehr & Technik. 2016. P. 49–62.
- Danilenko E. I. Zaliznychna kolya. Ulashtuvannia, proektuvannia i rozrakhunky, vzaiemodiya z rukhomym skladom. Vol. 1. Kyiv: Inpres, 2010. 528 p.
- Harantiyni stroky sluzhby ta umovy zabezpechennia harantiynoi ekspluatatsiyi metalevykh elementiv strilochnykh perevodiv / Danilenko E. I., Karpov M. I., Boiko V. D. et. al. Kyiv: Transport Ukrainy, 2007. 56 p.
- Polozhennia pro normatyvni stroky sluzhby strilochnykh perevodiv u riznykh ekspluatatsiynykh umovakh. Kyiv: Transport Ukrainy, 2003. 30 p.
- Concluding Technical Report. INNTRACK, Innovative Track Systems. URL: <http://www.charmec.chalmers.se/innotrack/>
- Evaluation of the stressed-strained state of crossings of the 1/11 type turnouts by the finite element method / Kovalchuk V., Bolzhelarskiy Y., Parneta B., Pentsak A., Petrenko O., Mudryy I. // Eastern-European Journal of Enterprise Technologies. 2017. Vol. 4, Issue 7 (88). P. 10–16. doi: <https://doi.org/10.15587/1729-4061.2017.107024>
- TU U 27.3-26524137-1340:2005. Khrestovyny zaliznychni staroprydatni vidremontovani v kolyi naplavkoiu. Derzhavna administratsiya zaliznychnoho transportu Ukrainy. Kyiv: VD «Manufaktura», 2006. 40 p.
- Simulation of wheel-rail contact and subsequent material degradation in switches & crossings / Nicklisch D., Nielsen J. C. O., Ekh M., Johansson A., Pålsson B., Zoll A., Reinecke J. // Proceedings of the 21st International Symposium on Dynamics of Vehicles on Roads and Tracks (IAVSD). Stockholm, Sweden, 2009.
- The study of strength of corrugated metal structures of railroad tracks / Kovalchuk V., Markul R., Bal O., Milyanych A., Pentsak A., Parneta B., Gajda A. // Eastern-European Journal of Enterprise Technologies. 2017. Vol. 2, Issue 7 (86). P. 18–25. doi: <https://doi.org/10.15587/1729-4061.2017.96549>
- Dynamical response of railway switches and crossings / Salajka V., Smolka M., Kala J., Plášek O. // MATEC Web of Conferences. 2017. Vol. 107. P. 00018. doi: <https://doi.org/10.1051/mateconf/201710700018>
- Estimation of carrying capacity of metallic corrugated structures of the type Multiplate MP 150 during interaction with backfill soil / Kovalchuk V., Kovalchuk Y., Sysyn M., Stankevych V., Petrenko O. // Eastern-European Journal of Enterprise Technologies. 2018. Vol. 1, Issue 1 (91). P. 18–26. doi: <https://doi.org/10.15587/1729-4061.2018.123002>
- Kassa E. Dynamic train-turnout interaction: mathematical modelling, numerical simulation and field testing: PhD Thesis, Department of Applied Mechanics. Chalmers University of Technology, Göteborg, 2007.
- Study of the stress-strain state in defective railway reinforced-concrete pipes restored with corrugated metal structures / Kovalchuk V., Markul R., Pentsak A., Parneta B., Gayda O., Braichenko S. // Eastern-European Journal of Enterprise Technologies. 2017. Vol. 5, Issue 1 (89). P. 37–44. doi: <https://doi.org/10.15587/1729-4061.2017.109611>
- Myamlin S. V. Modelirovanie dinamiki rel'sovoyh ekipazhey. Dnepropetrovsk: Novaya ideologiya, 2002. 240 p.
- Alad'ev V. Z., Bogdyavichyus M. A. MAPLE 6: Reshenie matematicheskikh, statisticheskikh i fiziko-tekhnicheskikh zadach. Moscow: Laboratoriya Bazovyh Znaniy, 2001. 824 p.
- Met'yuz D. G., Fink K. D. Chislennye metody. Ispol'zovanie MATLAB. 3-e izd. Moscow: Izdatel'skiy dom «Vil'yams», 2001. 720 p.
- Gule Zh. Soprotivlenie materialov: sprav. pos. Moscow: Shkola, 1985. 193 p.